



HAL
open science

An anhydrous high-pressure synthesis route to rutile type RhO₂

G rard Demazeau, Alexey Baranov, Rainer P ttgen, Lorenz Kienle, Manfred
H. M ller, Rolf-Dieter Hoffmann, Martin Valldor

► **To cite this version:**

G rard Demazeau, Alexey Baranov, Rainer P ttgen, Lorenz Kienle, Manfred H. M ller, et al.. An
anhydrous high-pressure synthesis route to rutile type RhO₂. Zeitschrift fur Naturforschung B, 2006,
61 (12), pp.1500-1506. 10.1515/znb-2006-1206 . hal-00123302

HAL Id: hal-00123302

<https://hal.science/hal-00123302>

Submitted on 20 Feb 2024

HAL is a multi-disciplinary open access archive for the deposit and dissemination of scientific research documents, whether they are published or not. The documents may come from teaching and research institutions in France or abroad, or from public or private research centers.

L'archive ouverte pluridisciplinaire **HAL**, est destin e au d p t et   la diffusion de documents scientifiques de niveau recherche, publi s ou non,  manant des  tablissements d'enseignement et de recherche fran ais ou  trangers, des laboratoires publics ou priv s.

An Anhydrous High-pressure Synthesis Route to Rutile Type RhO_2

G rard Demazeau^a, Alexis Baranov^{a,b}, Rainer P ttgen^c, Lorenz Kienle^d,
Manfred H. M ller^c, Rolf-Dieter Hoffmann^c, and Martin Valldor^e

^a Institut de Chimie de la Mati re Condens e de Bordeaux, Centre de Ressources Hautes Pressions (ICMCB–CNRS and ENSCPB), Universit  Bordeaux I ‹‹Sciences et Technologies››, 87 Avenue du Docteur A. Schweitzer, 33608 Pessac Cedex, France

^b Department of Chemistry, Lomonosov University, 119992 Moscow, Russia

^c Institut f r Anorganische und Analytische Chemie, Westfalische Wilhelms-Universitt M nster, Corrensstra e 30, 48149 M nster, Germany

^d Max-Planck-Institut f r Festk rperforschung, Heisenbergstra e 1, 70569 Stuttgart, Germany

^e Institut f r Physik der Kondensierten Materie, Technische Universitt Braunschweig, Mendelssohnstra e 3, 38106 Braunschweig, Germany

Reprint requests to R. P ttgen. E-mail: pottgen@uni-muenster.de

Z. Naturforsch. **61b**, 1500–1506 (2006); received June 3, 2006

A new anhydrous high-pressure synthesis route was developed for rutile type RhO_2 . Rhodium(III) chloride was reacted with Na_2O_2 at 600  C under an oxygen pressure of 200 MPa yielding RhO_2 and NaCl. X-ray powder diffractometer data and TEM observations confirmed the rutile structure: $P4_2/mnm$, $a = 448.7(1)$, $c = 308.9(1)$ pm, $x(\text{O}) = 0.3125(8)$, leading to Rh–O distances of 195.0 (4 ) and 198.3 pm (2 ) in the slightly elongated octahedra. Structural transformations associated with the production of oxygen vacancies can be initiated by electron-beam heating.

Key words: High-pressure Synthesis, Crystal Chemistry

Introduction

The rutile structure, space group $P4_2/mnm$ (Fig. 1) is one of the basic inorganic structure types [1–3]. Many binary oxides MO_2 ($M = \text{Si, Ge, Sn, Pb, Ti, Cr, Mn, Ta, Tc, Re, Ru, Rh, Os, Ir, Te}$) and fluorides MF_2 ($M = \text{Mg, Mn, Fe, Co, Ni, Zn, Pd}$) adopt this structure. Among the many MO_2 compounds, rutile type TiO_2 has the by far broadest technical application. It is produced in enormous tonnages as white pigment in paints and floor polishes [4]. CrO_2 , one of the few oxides ferromagnetic at r. t., has for a long time been used as magnetic recording material for tapes.

While many MO_2 oxides and the MF_2 fluorides can be synthesized under ambient pressure conditions, some of them, especially SiO_2 (stishovite) [5–7], CrO_2 [8,9], and RhO_2 [10–13], are only accessible using high oxygen pressures. In the original work by Muller and Roy [12], RhO_2 was prepared from the precursor $\text{Rh}_2\text{O}_3 \cdot 5\text{H}_2\text{O}$ under high oxygen pressures. A severe disadvantage of this precursor is the formation of RhOOH [14, 15] as a side product.

So far, only resistivity data at r. t. and 4.2 K on a $\text{Rh}_2\text{O}_3/\text{RhO}_2$ mixture have been reported by Shannon [11]. We were interested in the chemi-

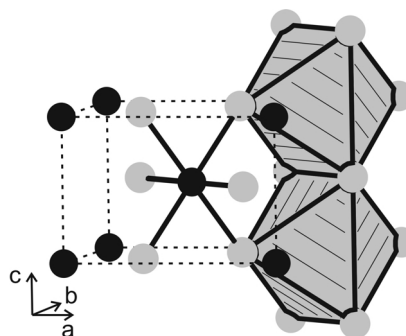


Fig. 1. The rutile type structure of RhO_2 , space group $P4_2/mnm$. The rhodium and oxygen atoms are drawn as black and grey circles, respectively. The edge-sharing $\text{RhO}_6/3$ octahedra are emphasized.

cal bonding peculiarities and the physical properties of pure RhO_2 . Thermogravimetric analysis of RhO_2 samples prepared from $\text{Rh}_2\text{O}_3 \cdot 5\text{H}_2\text{O}$ suggested that some hydroxyl groups could be present in the rutile structure leading to a stabilization of a mixed valence situation for rhodium ($\text{Rh}^{4+}/\text{Rh}^{3+}$) according to $[\text{Rh}^{4+}_{1-x}\text{Rh}^{3+}_x\text{O}_{2-x}(\text{OH})_x]$.

Consequently, in order to prepare pure RhO_2 , it was necessary to select a rhodium precursor free of water

or hydroxyl groups. Herein, we report on the synthesis of RhO₂ from RhCl₃ and Na₂O₂ under high oxygen pressure. The RhO₂ structure has been characterized *via* powder X-ray diffraction and high resolution transmission electron microscopy.

Experimental Section

Synthesis

Starting materials for the different preparation routes involving RhO₂ were Rh₂O₃ · xH₂O ($x \approx 5$) (Aldrich), anhydrous RhCl₃ (98%, Aldrich) and Na₂O₂ (97%, Aldrich). The double stage equipment of gas compression (in particular oxygen) set up in Bordeaux [16] was used.

Three different preparation routes have been evaluated:

(i) The conventional one corresponding to that described by Muller and Roy [12] using Rh₂O₃ · xH₂O ($x \approx 5$) treated under high oxygen pressure (200 MPa) at 600 °C during 48 h (sample 1).

(ii) The second route involving anhydrous RhCl₃ as precursor under similar reaction conditions (a high oxygen pressure of 200 MPa at $T = 600$ °C for 48 h) leading to the formation of RhO₂ (as detected *via* X-ray powder diffraction).

In order to avoid the incorporation of chloride ions into the rutile structure of rhodium dioxide, a third process was evaluated:

(iii) In order to trap Cl⁻ and to maintain the oxidizing conditions Na₂O₂ was used thoroughly mixed with RhCl₃ in stoichiometric proportions: $2\text{RhCl}_3 + 3\text{Na}_2\text{O}_2 \rightarrow 2\text{RhO}_2 + 6\text{NaCl} + \text{O}_2$. In a first step the reaction mixture was treated under argon pressure using always the same experimental conditions, *i. e.* $p = 200$ MPa, $T = 600$ °C, $t = 48$ h. The resulting products were NaCl, Rh₂O₃, and elemental rhodium. This result suggested that thermal decomposition of Na₂O₂ and NaCl formation take place at lower temperature than that required for oxidation of rhodium to Rh⁴⁺. Consequently, instead of argon, oxygen pressure was employed using the same thermodynamic conditions (200 MPa, 600 °C, 48 h). Under such conditions pure RhO₂ and NaCl were the resulting products (detected *via* X-ray powder diffraction). Scanning electron microscopy revealed a lath-shaped habit for the RhO₂ crystals (sample 2).

X-ray powder data

The samples were characterized on a Stoe StadiP powder diffractometer with CuK_{α1} radiation ($\lambda = 154.0598$ pm, Ge monochromator) and silicon ($a = 543.07$ pm) as an external standard. To ensure correct indexing, the observed patterns were compared with calculated ones [17], taking the atomic positions obtained from the structure refinements. The lattice parameters were subsequently refined through least-squares fits. The experimental powder diffractograms of the RhO₂ samples prepared from the precursors Rh₂O₃ · 5H₂O and

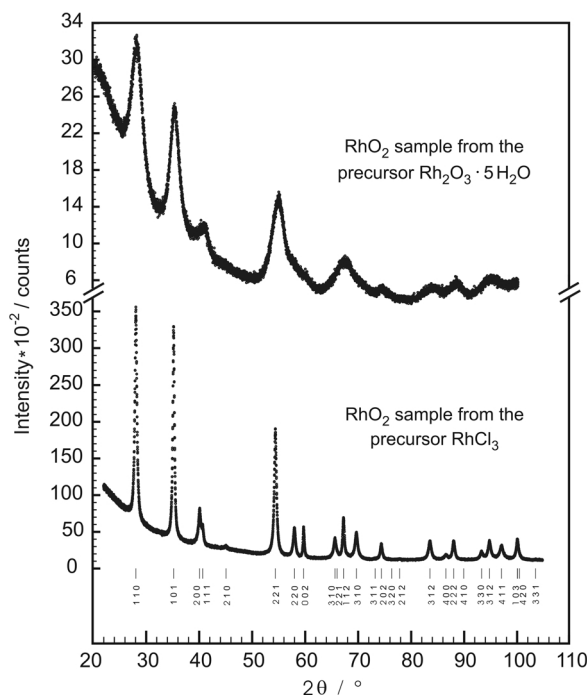


Fig. 2. X-ray powder diffractograms (CuK_{α1} radiation) of RhO₂ samples prepared from the precursors Rh₂O₃ · 5H₂O (top) and RhCl₃ (bottom). The hkl indices are also listed.

RhCl₃ are presented in Fig. 2. From the two diagrams it is evident that the two samples have different particle sizes. The pattern of the RhO₂ sample prepared from Rh₂O₃ · 5H₂O has much larger line widths and several overlapping reflections cannot be resolved. Evaluation of the reflections half width according to the Scherrer formula indicates particle sizes of 4.0 ± 0.5 nm, which is in very good agreement with the HRTEM investigations discussed below.

The sample prepared from RhCl₃ as precursor has a much better crystallinity and shows sharp and well resolved reflections in the X-ray powder pattern (Fig. 2 bottom). Although the resolution of the pattern seems to be good, we could not get satisfactory Rietveld refinements for this and other samples. The profiles were not satisfactory, most likely due to preferred orientation and to internal stress within the samples prepared under high-pressure high-temperature conditions. Nevertheless, these refinements revealed an x parameter for the oxygen atoms of $x(\text{O}) = 0.3125(8)$.

The refined lattice parameters are $a = 448.9(8)$ and $c = 309.4(6)$ pm for the sample obtained from the Rh₂O₃ · 5H₂O precursor as compared to $a = 448.7(1)$ and $c = 308.9(1)$ pm for the sample prepared from RhCl₃. The lower resolution of the first diagram manifests itself also in the larger standard deviations of the lattice parameters. The present data are in excellent agreement with those originally reported by Muller and Roy [12].

Thermogravimetry

Thermogravimetry was performed in flowing N₂ (ca. 50 mL/h) in the temperature range 20–1300 °C using a SETARAM TAG24 setup. 17.02 mg of the sample were placed in a corundum sample holder and the temperature was raised with a rate of 10 °C/min.

Electron microscopy

HRTEM (high resolution transmission electron microscopy) and SAED (selected area electron diffraction) investigations were performed with a Philips CM30ST (300 kV, LaB₆ cathode, C_S = 1.15 mm). Computer simulations of the HRTEM images (multislice formalism) and SAED patterns (kinematical approximation) were carried out with the EMS program package [18] (spread of defocus: 70 Å, illumination semiangle: 1.2 mrad). All images were collected with a Multiscan CCD Camera (software Digital Micrograph 3.6.1 (Gatan)). EDX (energy dispersive X-ray spectroscopy) was performed in the scanning- and nanoprobe mode of CM30ST with a Si/Li-EDX detector (Noran, Vantage System).

Discussion

Synthesis conditions

The syntheses were started with Rh₂O₃ · 5H₂O as precursor compound. The latter was treated under high oxygen pressures (up to 350 MPa, 400–600 °C). Thermogravimetric data (Fig. 3) of this sample clearly revealed a water content, most likely due to RhOOH and a solid solution (Rh⁴⁺_(1-x)Rh³⁺_xO_(2-x)OH_x) with rutile structure. These findings were in good agreement with the studies carried out by Moran-Miguel and Alario-Franco [13] and Chenavas *et al.* [14]. After decomposition to Rh₂O₃, a further rhodium oxide with minor oxygen content is observed as intermediate phase. Similar rhodium oxide species have been observed during the progressive oxidation of rhodium clusters on alumina [19].

In order to prevent the participation of OH groups in the formation of the RhO₂ structure, it was necessary for preparing RhO₂ to take into account two prerequisites, (i) oxidizing conditions and (ii) a precursor without any H₂O or OH groups. RhCl₃ was selected as precursor and Na₂O₂ as an oxidant. Due to the low thermal stability of Na₂O₂, its decomposition takes place prior to the rhodium III → IV oxidation. Consequently this reaction was carried out under high oxygen pressure (200 MPa O₂ and 600 °C):

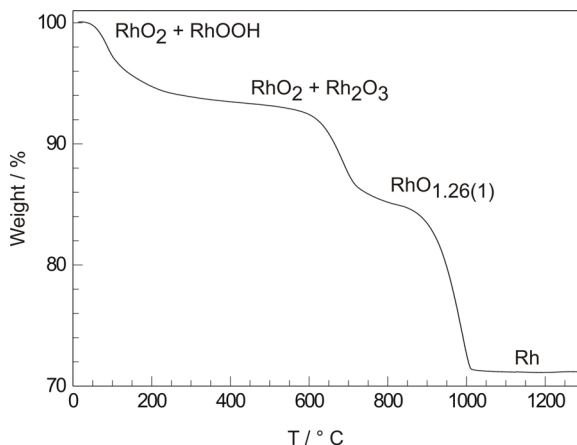


Fig. 3. Thermogravimetric analysis of the RhO₂ sample prepared from Rh₂O₃ · 5H₂O under high oxygen pressure. For details see text.

$2\text{RhCl}_3 + 3\text{Na}_2\text{O}_2 \rightarrow 2\text{RhO}_2 + 6\text{NaCl}$. Sodium chloride was washed out with distilled water, and X-ray pure rhodium dioxide was obtained by this preparation process.

Crystal chemistry

RhO₂ adopts the tetragonal rutile structure (Fig. 1). The rhodium atoms have octahedral oxygen coordination at Rh–O of 195.0 (4×) and 198.3 pm (2×). The RhO_{6/3} octahedra share common edges within the *c* direction and these strands are connected *via* common corners. In parallel to the polyhedral presentation, the rutile type structure of RhO₂ can also be derived from a tetragonal close packing [20] of the oxygen atoms. Here, each oxygen atom has eleven nearest oxygen neighbors at O–O distances ranging from 238 to 309 pm. The rhodium atoms fill the slightly distorted octahedral voids within that packing.

Further studies on the chemical bonding peculiarities and the magnetic and electrical properties of pure RhO₂ are in progress.

Electron microscopy

Samples 1 (precursor Rh₂O₃ · 5H₂O) and 2 (precursors RhCl₃/Na₂O₂) are characterized by distinct features of their morphology. For sample 1 the average size of the oval particles is about 5 nm, *cf.* Fig. 4a, top. SAED patterns recorded on aggregates of the nanoparticles exhibit concentric rings around 000 with almost homogeneous distribution of the diffracted intensity within one ring (Fig. 4b). This diffraction pat-

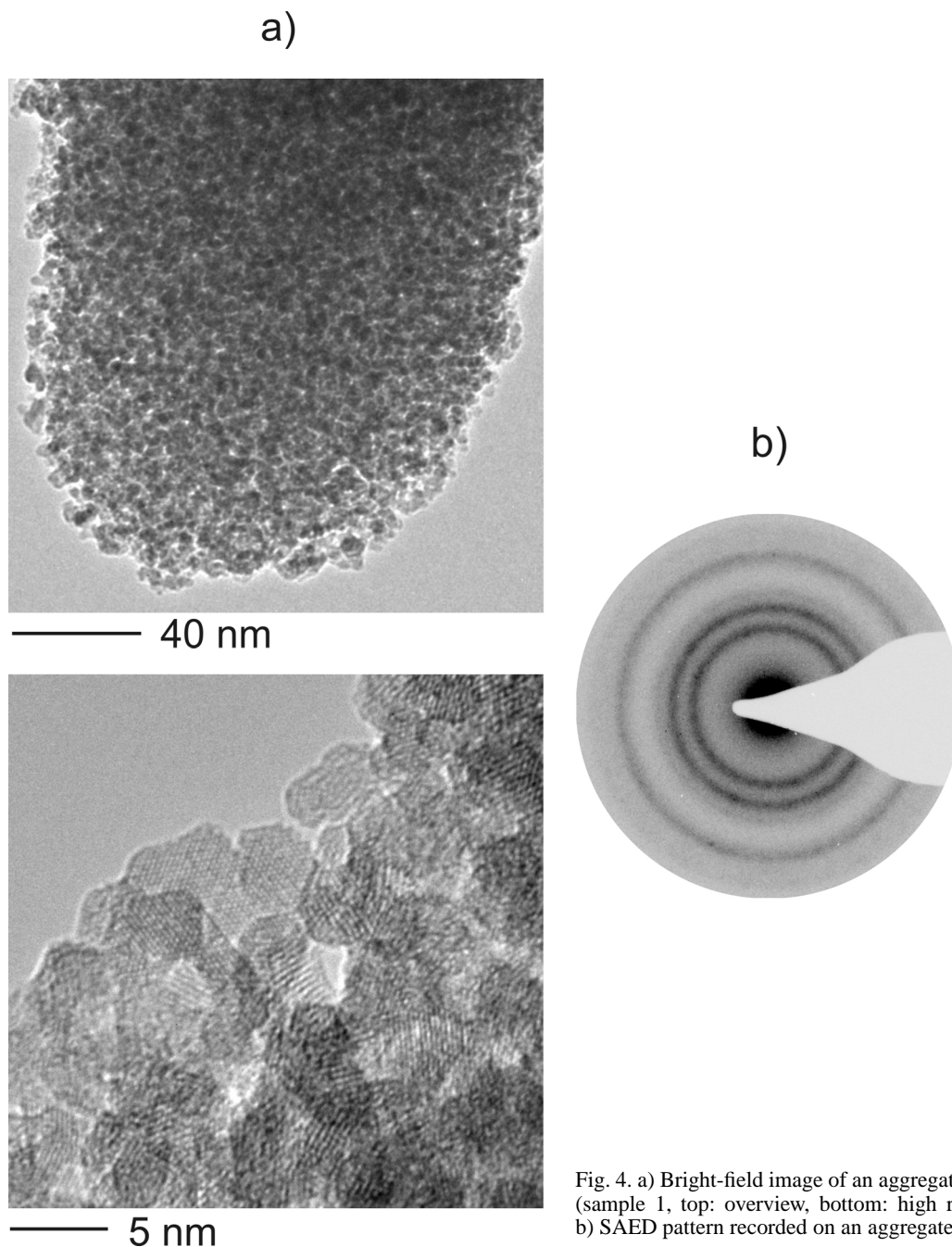


Fig. 4. a) Bright-field image of an aggregate of nanoparticles (sample 1, top: overview, bottom: high resolution image); b) SAED pattern recorded on an aggregate of nanoparticles.

tern correlates with the orientational disorder of highly crystalline but nanosized particles. The crystallinity can also be demonstrated by high resolution images (Fig. 4a, bottom). As shown by Fourier transformations, the equispaced stripes in the HRTEM micro-

graphs correlate with Miller planes. The d -values determined from diffraction patterns are consistent with a rutile type structure, *e. g.* $d_{110} \sim 3.2 \text{ \AA}$ (calc.: 3.17 \AA), $d_{101} \sim 2.5 \text{ \AA}$ (calc.: 2.54 \AA), $d_{200} \sim 2.2 \text{ \AA}$ (calc.: 2.25 \AA) and $d_{211} \sim 1.7 \text{ \AA}$ (calc.: 1.68 \AA).

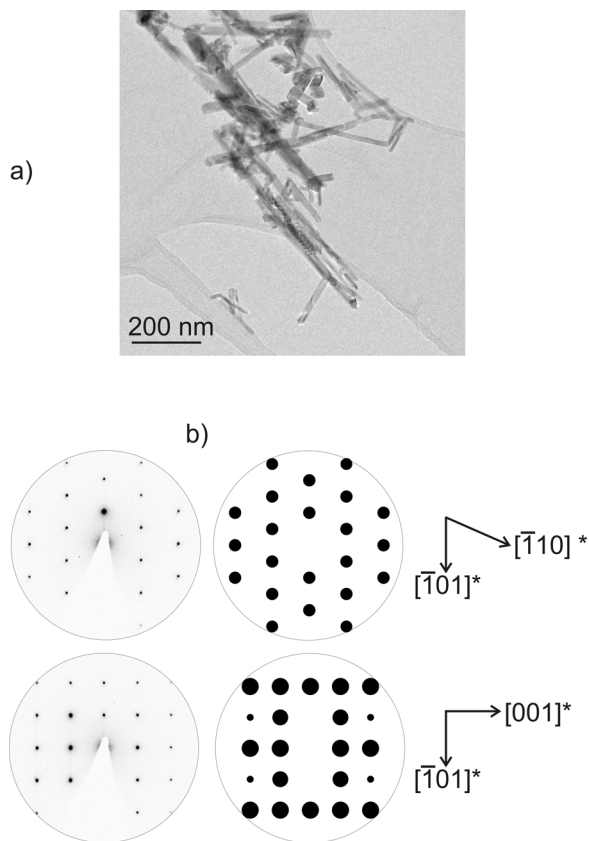


Fig. 5. Bright-field image of RhO_2 needles (sample 2); diffraction patterns of one needle (tilting experiment, see text), a) zone axis $[111]$, b) zone axis $[110]$ with simulated patterns (kinematical approximation).

For sample 2, only a minor fraction of nanoparticles was observed, while the majority consists of highly crystalline needles (Fig. 5a) with a typical width of 50 nm and a length of up to several microns. Series of SAED patterns obtained by tilting the needles systematically (Fig. 5b, top: zone axis $[111]$, bottom: zone axis $[110]$, experimental tilt angle \sim calculated tilt angle = 26°) confirm symmetry and lattice of a rutile type structure.

The HRTEM micrographs of Fig. 6 were recorded on an aligned needle of sample 2 (zone axis orientation $[111]$, variable defocus). Both micrographs show convincing agreement with simulations (see insets in Fig. 6). The contributions of the oxygen atoms to the image contrast are marginal, see projected potential (Fig. 6, bottom). Hence, defects in the oxygen substructure can only be detected if they are interconnected with changes in the arrangement of the rhodium

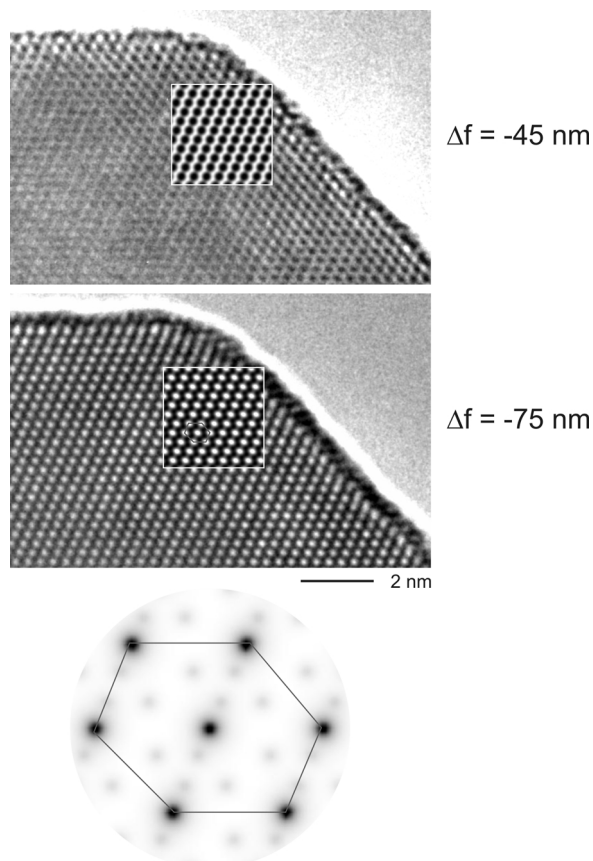
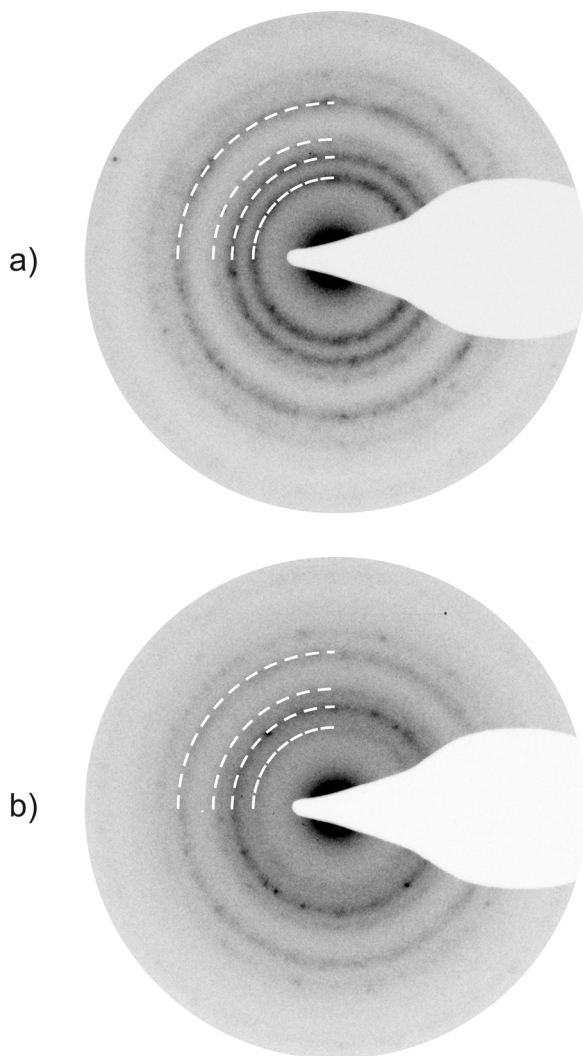


Fig. 6. Top: HRTEM micrographs of a RhO_2 needle with inserted simulations (sample 2, parameters for simulation: thickness: 3.5 nm, defocus values: see figure). Bottom: projected potential of RhO_2 , $[111]$.

atoms. Such deviations from the undistorted rutile type structure were never observed for the needles of sample 2. Both samples were tested for their sensitivity against electron beam irradiation, particularly, if heating of the samples by focusing the electron beam allows observing structural transformations *in situ*. Actually, sample 1 showed structural changes already under the moderate conditions usually selected for HRTEM. The intensity of the 110 reflection is strongly reduced and full extinction occurs after several minutes of irradiation (Fig. 7). Such transformation cannot be initiated on the rutile type needles of sample 2, even not by increasing the current density by a factor of 40. This is further proof for the OH^- content in the samples prepared from the $\text{Rh}_2\text{O}_3 \cdot 5\text{H}_2\text{O}$ precursor. The structural transformations of these samples are associated with the loss of water.



← Fig. 7. Effect of beam heating on diffraction patterns (sample 1): a) before beam heating, b) after two minutes of beam heating.

We assume that the rutile type structure of sample 1 transforms to an unknown structure. EDX analyses qualitatively indicate a reduction of the oxygen content during irradiation, finally leading to the formation of Rh metal after long term irradiation. The structure of the oxygen deficient phase cannot be determined by standard X-ray or electron microscopy techniques due to the nano size of the particles. However, a first hypothetical model of the defect RhO_{2-x} phase seems to be self-evident when taking into account the defect phases of the binary system Ti–O. In this case, defect phases with average rock salt type structure ($Fm\bar{3}m$) were described [21]. Such compounds were not characterized for the system Rh–O so far. However, the transformation into such structures would explain the extinction of the 110 reflection, since for a rock salt type the lowest d -value would be ~ 2.5 Å (111 reflection) coinciding with 101_{rutile} .

Acknowledgements

This work was supported by the Deutsche Forschungsgemeinschaft, the European Science Foundation through the COST D30 Program and CNRS (Department of Chemistry). The authors thank Mrs. V. Duppel for practical TEM work and Prof. Dr. Dr. h. c. mult. A. Simon for enabling the TEM experiments. Prof. M. Nygren at Stockholm University is acknowledged for running the TG experiments.

- [1] D.M. Adams, *Inorganic Solids*, John Wiley & Sons, London (1974).
- [2] U. Müller, *Anorganische Strukturchemie*, Teubner, Stuttgart (1996).
- [3] W.H. Baur, *Z. Kristallogr.* **209**, 143 (1994).
- [4] W. Büchner, R. Schliebs, G. Winter, K.H. Büchel, *Industrielle Anorganische Chemie*, VCH, Weinheim (1986).
- [5] S.M. Stishov, N.V. Belov, *Dokl. Akad. Nauk SSSR* **143**, 951 (1962).
- [6] V. Srikanth, R. Roy, E.K. Graham, D.E. Voigt, *J. Am. Chem. Soc.* **74**, 3145 (1991).
- [7] J.M. Leger, J. Haines, M. Schmidt, J.P. Petit, A.S. Pereira, J.A.H. de Jomada, *Nature* **383**, 401 (1996).
- [8] G. Demazeau, P. Maestro, Th. Plante, M. Pouchard, P. Hagenmuller, *Mater. Res. Bull.* **14**, 121 (1979).
- [9] G. Demazeau, P. Maestro, Th. Plante, M. Pouchard, P. Hagenmuller, *J. Phys. Chem. Solids* **41**, 1139 (1980).
- [10] L. Wöhler, K.F.A. Ewald, *Z. Anorg. Allg. Chem.* **201**, 145 (1931).
- [11] R.D. Shannon, *Solid State Commun.* **6**, 139 (1968).
- [12] O. Muller, R. Roy, *J. Less-Common Met.* **16**, 129 (1968).
- [13] E. Moran-Miguel, M.A. Alario-Franco, *Thermochim. Acta* **60**, 181 (1983).
- [14] J. Chenavas, J.C. Joubert, J.J. Capponi, M. Marezio, *J. Solid State Chem.* **6**, 1 (1973).
- [15] E. Moran-Miguel, M.A. Alario-Franco, *J. Solid State Chem.* **46**, 156 (1983).
- [16] G. Demazeau, Thèse de doctorat es Sciences Physiques, Université Bordeaux 1 (France), N° 419 (1973).

- [17] K. Yvon, W. Jeitschko, E. Parthé, *J. Appl. Crystallogr.* **10**, 73 (1977).
[18] P. A. Stadelmann, *Ultramicroscopy* **21**, 131 (1987).
[19] C.-P. Hwang, C.-T. Yeh, Q. Zhu, *Catalysis Today* **51**, 93 (1999).
[20] W. H. Baur, *Mater. Res. Bull.* **16**, 339 (1981).
[21] V. Dufek, F. Petru, V. Brozek, *Monatsh. Chem.* **98**, 2424 (1967).